CCUS: 4443712

Implications of Geochemical Alteration (Mineralization, Precipitation, and Dissolution) on Relative Permeability of the CO_2 Brine Rock System for Long-Term CO_2 Storage and Monitoring in the Silurian Dolomite Formation, Permian Basin

Muhammad Noman Khan*[1], Brian McPherson[2], Shameem Siddiqui[1], Nathan Moodie[2], Ganesh C. Thakur[1], Mike Myers[1], Lori Hathon[1] ,
1. University of Houston, 2. University of Utah

This paper was prepared for presentation at the Carbon Capture, Utilization, and Storage conference held in The Woodlands, TX, 30 March – 01 April.

Abstract

Understanding the coupled geochemical and flow behavior of CO_2 in subsurface formations is critical for predicting the long-term performance of CCUS projects. This study presents an integrated experimental workflow designed to evaluate how mineralization, precipitation, and dissolution may influence the relative permeability of the CO_2-brine-rock system in Silurian dolomite of the Permian Basin, a region with significant potential for large-scale CO_2 storage. This work outlines an experimental and analytical framework for assessing how uncertainties in geochemical processes can affect two-phase flow properties, with a particular focus on how these processes alter porosity, permeability, and fluid mobility.

A comprehensive workflow was employed, including core scale flow tests under ambient and reservoir conditions. Porosity and permeability were measured using standard porosimeter and permeameter, along with micro-CT imaging, thin sections, and NMR, to characterize pore structures. Core flooding experiments were conducted with the AFS 300 Coreflooding system at 90 °C and at elevated pressures, using a 20 wt% NaCl brine and $scCO_2$, before and after long-term exposure, to assess time-dependent geochemical alterations. Relative permeability measurements were conducted as part of the workflow, providing baseline data to support subsequent analysis of geochemically driven changes.

Preliminary petrophysical observations indicate that mineralization and precipitation are associated with reduced pore connectivity and fluid mobility, while dissolution processes may enhance injectivity

but may create unstable flow paths. These competing processes have significant implications for CO_2 plume migration and storage security. By linking geochemical reactions to dynamic flow behavior, this study provides novel insights into the design, monitoring, and risk assessment of CCS operations in carbonates. The results of this work can be used in upscaled reservoir simulation models for future CO_2 sequestration projects.

This advanced technique enhances reservoir characterization by analyzing pore geometry and pore texture, and evaluating the implications of the relative permeability of CO_2 and brine on geochemical processes. It significantly improves the outcomes of CO_2 sequestration in the pore space. This study establishes the experimental basis for correlating geochemical alteration with CO_2–brine relative permeability in future analyses, and it will be of immense value in understanding the complexities of rock-fluid interactions in carbon sequestration projects in similar lithologies.

Introduction

Relative permeability has been recognized as a fundamental reservoir property since 1936 (Wyckoff and Botset, 1936). Despite nearly 90 years of research evolution, challenges remain in integrating geochemical alteration with multiphase flow characterization. This work aims to support the evaluation of Class VI well performance by addressing the scientific gap between geochemical reactions, porosity evolution, and relative permeability of the $scCO_2$-brine-rock system. Geochemical alteration plays a critical role in CCS and CCUS flow behavior, as mineralization, precipitation, and dissolution processes can significantly impact petrophysical properties and multiphase flow characteristics during geological CO_2 storage. This study is part of the DOE CarbonSAFE project, focusing on the Silurian dolomite formation in the Permian Basin. The objective of this study is to develop and demonstrate an experimental workflow capable of evaluating the implications of geochemical alteration (mineralization, precipitation, and dissolution (MPD)) on the relative permeability of the $scCO_2$-brine-rock system for long-term CO_2 storage and monitoring. Previous studies, including Khan et al. (2024, 2025), demonstrated that MPD processes alter petrophysical properties through mineralogical and geochemical changes during CO_2–brine–rock interactions, both in core-flooding and static batch reactor experiments. Other researchers have shown that porosity and permeability respond to changes in pore structure, to petrophysical properties influenced by heterogeneities, and to mineral dissolution and precipitation processes (Wang et al., 2021). Understanding CO_2 storage in saline aquifers requires integrating geochemical reactions and multiphase flow behavior. While reactive transport studies use specific surface area (SSA) to control reaction rates, multiphase flow investigations often ignore SSA and pore-structure evolution. To date, few studies have attempted to explicitly link SSA-driven geochemical changes with relative permeability behavior. This study lays the groundwork for addressing that gap through an integrated experimental workflow by linking reactive surface changes to multiphase flow behavior.

We investigate geochemical alteration mechanisms in the Fusselman Silurian dolomite formation and establish a connection between the evolution of dynamic specific surface area (SSA) and relative permeability (Kr). SSA governs mineral reaction rates and pore-geometry evolution, which are critical for predicting long-term CO_2 storage performance. Geochemical reactions continuously reshape pore networks, yet relative permeability is often assumed static, creating a contradiction with pore-scale evolution. This study proposes and demonstrates a workflow linking SSA-relevant pore-structure evolution driven by MPD processes to relative permeability analysis, providing a more realistic framework for evaluating long-term CO_2 storage behavior. This study proposes a new workflow linking SSA evolution driven by MPD processes to relative permeability, providing a more realistic framework for evaluating long-term CO_2 storage behavior.

A detailed literature review is presented in Tables 1,, tracing the development of relative permeability research, beginning with the pioneering work of Wyckoff & Botset, Buckley & Leverett, Hassler, Johnson, Bossler & Naumann (JBN), Corey, and many others, with continuous advancements in both steady-state and unsteady-state relative permeability analysis. Table 2 lists some of the important laboratory work done on CO_2-Brine-rock systems.

Table 1. Literature Review on Relative Permeability

Year	Author(s)	Key Findings
1936	Wyckoff & Botset	First experimental measurement of gas-liquid relative permeability in unconsolidated sands.
1942	Buckley & Leverett	Developed a theory for oil-water displacement, forming the basis for unsteady-state analysis.
1944	Hassler	Patented steady-state method for relative permeability using semi-permeable membranes.
1947	Morse et al.	Developed Penn State technique to reduce boundary effects using high-permeability core inserts.
1950	Gates & Lietz; Brownscombe et al.	Improved Hassler's method to reduce time and complexity.
1951	Osoba et al.; Caudle et al.	Further optimized the steady-state and Penn State methods.
1951	Rapoport & Leas	Introduced a scaling factor to minimize capillary effects in lab corefloods.
1952	Josendal et al.; Welge	Extended Buckley-Leverett theory into the Welge-JBN method for unsteady-state relative permeability.
1954	Corey	Developed Corey's correlations for modeling relative permeability and capillary pressure vs. saturation.
1959	Johnson et al.(JBN)	Provided analytical expansion of unsteady-state displacement methods, extending the work by Welge.
1978	Jones & Roszelle	Introduced a graphical approach to analyze relative permeability using Welge-JBN data.
1979	Sigmund & McCaffery	Advanced methods for interpreting displacement coreflood data.
1986	Honarpour et al.	Highlighted limitations of unsteady-state methods (heterogeneity, capillary effects, etc.).
1988	Watson et al.	Continued development of two-phase relative permeability analysis methods.

Table 2. Relative Permeability of CO_2-Brine-Rock System

Author (Year)	Objective	Rock Type	Method	Key Findings
Catriona et al. (2014)	Assess viscosity and flow rate.	Sandstone	Coreflood	Viscosity and rate control Kr behavior.
Patil (2015)	Link the Kr functions to mineral prediction.	Calcite cemented sandstone	Simulation	Accurate Kr is essential for reliable CO_2 sequestration models.
Chen et al. (2016)	Measure CO_2-brine Kr	Berea Sandstone	Steady-State	Long core minimized end effects.
AlQuraishi et al. (2017)	Evaluate CO_2-brine Kr in heterogeneous saline aquifers for CCS.	St. Peter, Knox, and Sylvania (Upper sandstone & Lower dolomite)	Steady & Unsteady-State	Low Krg values (0.064–0.186) linked to high residual brine saturation (0.251–0.431); rock heterogeneity (plug variation, layering) majorly affects displacement efficiency.
Bakhshian et al. (2020)	Explore anisotropy effects	Tuscaloosa Sandstone	Not specified	Anisotropy alters directional flow, which is critical for modeling.
Bai et al. (2020)	Study low-permeability scenarios	Not specified	Steady & Unsteady	Kr varies with miscible/immiscible CO_2 flooding.
Jeong et al. (2021)	Investigate the influence of flow rate.	Berea Sandstone	Steady-State	Flow rate affects Kr efficiency.
Matthieu et al. (2023)	Compare measurement methods	Fontainebleau Sandstone	Steady & Unsteady	Combined methods improve reliability.
Gao et al. (2023)	Study pressure effects	Berea Sandstone	Steady-State	Pressure impacts kr behavior significantly.
Ahmed et al. (2024)	Assess stability before/after storage.	Sandstone	Not specified	Kr remained stable.
Richardson et al. (2025)	Examine pressure/wettability effects.	Berea Sandstone	Steady-State	No significant impact on Kr; supports best practices.
Chai et al. (2025)	Analyze the permeability decline.	Sandstone	Steady-State	Reduction is linked to changes in pore structure.

Methodology

The experiments are being conducted on Silurian dolomite outcrop samples for preliminary results and on real reservoir samples from the Permian Basin. The reservoir samples are from two formations in the Klein #5 well:

1. Wristen Group Formation (depth: 10,721 – 10,721.5 ft)
2. 31 Formation (depth: 10,673.5 – 10,674 ft)

For each formation, two sets of samples were collected as part of a workflow intended to support relative permeability evaluation. All samples are horizontal plugs, as shown in Figure 1.

Figure 1. (a) Silurian dolomite outcrop sample. (b) 31 Formation, H1 horizontal plug, depth 10,673.5 – 10,674 ft. (c) 31 Formation, H2 horizontal plug, depth 10,673.5 – 10,674 ft. Both (b) and (c) samples have some vugs on the surface and inside. (d) Wristen Group Formation, H2 horizontal plug, depth 10,721 – 10,721.5 ft, showing vugs on the outer surface and micro-porosities.

The methodologies of this study are organized into the following distinct sections:

a) Core cleaning using toluene and methanol.

b) CT scanning using the industrial CT scanner YXLON FF20CT and the Xradia 510 Versa (Zeiss) micro-CT scanner, as shown in Figure 2 a.

c) Porosity and permeability measurements using Ultra-Pore and Ultra-Perm 600 equipment.

d) Saturate the samples to 100%.

e) Perform NMR measurements (including quick porosity, T_2, and T_1) to analyze pore structure, pore size, and pore volume.

f) Using the AFS300 Coreflooding System (Figure 2 b), conduct brine injection experiments to measure absolute permeability, followed by drainage experiments at ambient conditions (~300 psi pore pressure and ambient temperature).

g) After drainage, perform NMR and CT scans to observe residual water saturation.
h) Clean the sample and repeat steps b–e.

h) Using the AFS300 Coreflooding System, conduct brine injection experiments to measure absolute permeability at 1500 psi and 90 °C, followed by drainage experiments under the same conditions.
j) After drainage under reservoir conditions, perform NMR and CT scans to observe residual water saturation.

i) As shown in Figure 3, place the sample in a glass tube with ceramic frits, seal the tube and frit joints with heat-shrink Viton, and place the assembly in a static batch reactor at 120 °C and 4000 psi for 30 days.

j) Perform NMR and CT scans to observe changes after batch aging.

k) Repeat the experimental workflow starting from step a to step j.

All of these steps are very useful for observing geochemical changes using micro-CT and industrial CT. Micro-CT can be performed at the beginning and end of the experiments, including regions of interest (ROI), whereas industrial CT can be used during the experiments. Our main objective is to characterize changes in pore structure and SSA-relevant properties using NMR and CT measurements, providing inputs for future modeling and relative permeability analysis. These measurements will be valuable for the modeling component, supporting geochemical modeling to better understand relative permeability (Kr).

Figure 2. a) Industrial CT scanner YXLON FF-20, b) AFS300 Coreflooding System

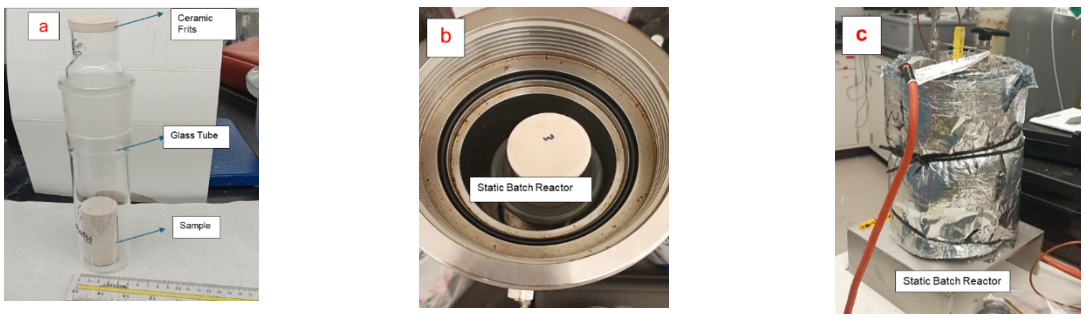

Figure 3. Sample assembly in a glass tube with ceramic frits, sealed with heat-shrink Viton, and aged in a static batch reactor at 120 °C and 4000 psi for 30 days.

Results and Discussions

The permeability and porosity of the Silurian dolomite sample are shown in Tables 3 and 4. The micro-CT scan of the Silurian dolomite, including the region of interest (ROI), was obtained using the Xradia micro-CT scanner. The Silurian dolomite sample was scanned prior to drainage experiments conducted as part of the relative permeability workflow experiment under ambient conditions.

Figure 4 shows CT-scan images of the Silurian dolomite sample after ambient-condition drainage during the Kr experiment and after reservoir-condition drainage at 90 °C and 1500 psi, respectively. No significant differences are observed at the CT scan resolution, indicating that pore-scale changes associated with drainage alone are limited under the tested conditions.

Tables 4 and 5 summarize the petrophysical measurements of the Silurian dolomite sample. Table 4 compares porosity and pore volume determined by helium porosimeter and NMR measurements, including quick porosity, T_2, and T_1. The results show good agreement between the methods, with porosity values ranging from 16.14% to 16.40% and pore volumes ranging from 13.995 to 14.345 mL, indicating the reliability of NMR measurements for characterizing the core. Table 5 presents the residual water saturation after reservoir-condition drainage, calculated from NMR measurements of T_1, T_2, and quick porosity. The residual water saturation values range from 24.2% to 27.2%, with the highest saturation observed in the quick porosity measurement. These results highlight NMR's ability to quantify residual fluids in the pore space following drainage experiments under reservoir conditions.

The NMR results, including quick porosity measurements, T_2, and T_1, are consistent with the other porosity measurements. However, after reservoir-condition drainage, the NMR results indicate residual water saturation, as reflected in the quick porosity, T_2, and T_1 responses. In the fully brine-saturated state, the NMR T2 distribution suggests on the order of 1.5% micro-porosity, 4% inter-particle porosity, and 9% vuggy porosity, applying standard cutoffs. After achieving irreducible water saturation, the observed T_2 distribution suggests that micropores remain fully saturated, and approximately 2% of capillary-bound water remains in inter-particle pores and vugs. All of the brine in the vuggy pores has been replaced with $scCO_2$.

Table 3. Petrophysical properties of the Silurian dolomite sample (before drainage experiment).

Property	Value
Dry weight	204.8 g
Pore volume (PV)	14.345 cc
Porosity	16.539 %
Length (L)	7.6396 cm
Diameter (D)	3.802 cm
Air permeability (Kair)	47 md
Klinkenberg permeability ($K\infty$)	29.280 md

Table 4. Petrophysical properties of the Silurian dolomite sample after the drainage experiment at ambient conditions.

Property	Value
Dry weight	204.369 g
Pore volume (PV)	14.714 cc
Porosity	16.965 %
Length (L)	7.6396 cm
Diameter (D)	3.802 cm
Air permeability (Kair)	47.2 md
Klinkenberg permeability ($K\infty$)	30 md

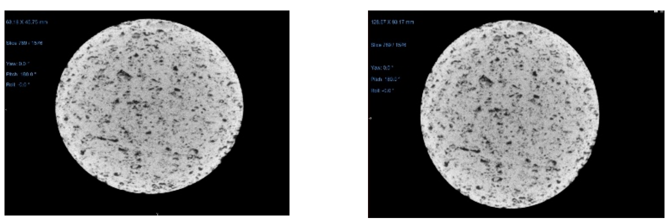

Figure 5. CT scan of Silurian dolomite after the drainage experiment: (a) at ambient conditions; (b) at reservoir conditions.

Table 4. Comparison of porosity and pore volume (PV) measured by NMR and helium porosimeter.

Test	Helium (%)	Quick Porosity (%)	T_2 (ml)
Pore Volume (ml)	14.345	14.228	13.995
Porosity (%)	16.36	16.40	16.14

Table 5. Residual water saturation of Silurian dolomite after reservoir-condition drainage experiment.

Measurement	Original Volume (mL)	Residual Water Volume (mL)	Residual Water Saturation (%)
T_1	14.039	3.399	24.2
T_2	13.995	3.585	25.6
Quick porosity	14.228	3.874	27.2

Conclusions

A New Pathway for Understanding CO_2 Flow Behavior

This study establishes and demonstrates an integrated experimental workflow for evaluating how geochemical alteration may influence multiphase flow behavior in Silurian dolomite-scCO_2-brine systems. CO_2-brine-rock reactions alter porosity, specific surface area (SSA), and pore connectivity, directly influencing relative permeability (Kr). Because SSA-driven pore-structure evolution is expected to influence relative permeability, quantifying this relationship represents an important objective of ongoing work, yet it has not been done previously. This study introduces a new workflow integrating CT imaging, NMR, coreflood experiments, post-flood aging, and SSA-driven modeling to capture these dynamics. The workflow presented here is designed to support future TOUGHREACT simulations aimed at generating time-dependent relative permeability curves, providing a more realistic framework for predicting CO_2 flow and storage behavior. These findings provide important insights into reservoir simulation, monitoring strategies, and the security of long-term CO_2 storage in CCS and CCUS projects in the Permian basin.

Acknowledgement

Funding for this work is provided by the U.S. Department of Energy's (DOE) National Energy Technology Laboratory (NETL) under Award No. DE-FE0032452. The authors gratefully acknowledge this financial support, as well as the support from the University of Houston Department of Petroleum Engineering.

Disclaimer

References

Ahmed, M.E.M., D.M. Paker, A. Abdulwarith, B. Dindoruk, S. Drylie, and S. Gautam (2024). "Quantification of the Effect of CO2 Storage on CO2-Brine Relative Permeability in Sandstone Reservoirs: An Experimental and Machine Learning Study (2024)." Paper presented at the SPE Annual Technical Conference and Exhibition, New Orleans, Louisiana, USA, September 2024.

AlQuraishi, A.A., S. Siddiqui, and O.A. Algadi (2017). "Influence of heterogeneities on CO2 sequestration in potential saline formations." In Offshore Mediterranean Conference and Exhibition, Ravenna, Italy, March 2017. Paper No. OMC-2017-512.

Bai, Mingxing, L. Liu, C. Li, and K. Song (2020). "Relative permeability characteristics during carbon capture and sequestration process in low-permeable reservoirs." Materials 13, no. 4 (2020): 990.

Bakhshian, S., S.A. Hosseini, and L.W. Lake (2020). "CO2-brine relative permeability and capillary pressure of Tuscaloosa sandstone: Effect of Anisotropy." Advances in Water Resources, Vol. 135 (2020): 103464.

Brownscombe, E. R., R.L. Slobod, and B.H. Caudle (1950). "Laboratory Determination of Relative Permeability," Oil and Gas Journal, Vol. 48, p. 98.

Buckley, S. E. and Leverett, M. C. (1942). "Mechanism of Fluid Displacement in Sands," Petroleum Transactions, A.I.M.E., Vol. 146, 1942, p. 107.

Chai, R., Q. Ma, S. Goodarzi, F.Y. Yow, B. Bijeljic, and M.J. Blunt (2025)."Multiphase Reactive Flow During CO2 Storage in Sandstone." Engineering, Vol. 48, May 2025, pp. 81-91.

Chen, X., A. Kianinejad, and D.A. DiCarlo (2017). "Measurements of CO2-brine relative permeability in Berea sandstone using pressure taps and a long core." Greenhouse Gases: Science and Technology, Vol. 7, Issue 2, pp. 370-382.

Corey, A.T. (1954). "The interrelation between gas and oil relative permeabilities." Producers Monthly, Vol. 19 (November), pp. 38-41.

Gao, B., E. Lyons, D. Magzymov, L. Poore, G. Besil, S. Richardson, and L. Lun (2023). "Steady-state supercritical CO2 and brine relative permeability measurements at different pressure conditions." In Symposium of the Society of Core Analysts. 2023.

Hassler, G. L. (1944). "Method and Apparatus for Permeability Measurements," U.S. Patent 2,345,935, April.

Honarpour, M., L. Koederitz, and A.H. Harvey (1986). Relative Permeability of Petroleum Reservoirs, Second Printing, CRC Press, Inc., Boca Raton, Florida.

Jeong, G.S., S. Ki, D.S. Lee, and I. Jang (2021). "Effect of the flow rate on the relative permeability curve in the CO2 and brine system for CO2 sequestration." Sustainability, Vol. 13, No. 3 (2021): 1543.

Johnson, E.F., Bossler, D.P. and Naumann, V.O. (1959). "Calculation of Relative Permeability from Displacement Experiments," Petroleum Transactions, A.I.M.E., Vol. 216, pp. 370-372.

Jones, S.C. and W.O. Roszelle (1978). "Graphical Techniques for Determining Relative Permeability from Displacement Experiments," Journal of Petroleum Technology, May 1978, p. 807.

Josendal, V.A., B.B. Sandiford and J.W. Wilson (1952). "Improved Multiphase flow Studies Employing Radioactive Tracers," Petroleum Transactions, A.I.M.E., Vol. 195, pp. 65-76.

Kerig, P.D. and A.T. Watson (1987). "A New Algorithm for Estimating Relative-Permeabilities from Displacement Experiments," SPE Reservoir Engineering, February, pp. 103-112.

Khan, M.N., S. Siddiqui, and G.C. Thakur (2024). "Recent advances in geochemical and mineralogical studies on CO2–brine–rock interaction for CO2 sequestration: Laboratory and simulation studies." *Energies* 17, no. 13 (2024): 3346.

Mascle, M., A. Oisel, P.K. Munkerud, E. Ebeltoft, O. Lopez, C. Pryme, and S. Youssef (2025). "CO2/Brine Relative Permeability Measurements at Reservoir Conditions: How to Reconciliate SS and USS Methods?." Petrophysics-The SPWLA Journal, Vol.66, No. 01 (2025), pp. 26-43.

Morse, R.A., P.L. Terwilliger, and S.T. Yuster (1947). "Relative Permeability Measurements on Small Samples," Producers Monthly, August,, pp. 19-25.

Osoba, J. S., J.G. Richardson, J.K. Kerver, J.A. Hafford and P.M. Blair (1951). "Laboratory Measurements of Relative Permeability," SPE 951047-G, Petroleum Transactions, A.I.M.E., Vol. 192, pp. 47-61.

Patil, V.V. "Self-sealing of faults in geological carbon sequestration." PhD diss., The University of Utah, 2016.

Rapoport L.A. and W.J. Leas (1951). "Relative Permeability to Liquid in Liquid-Gas Systems," Petroleum Transactions, A.I.M.E., Vol. 192, 1951, p. 83.

Reynolds, C., M. Blunt, and S. Krevor (2014). "Impact of reservoir conditions on CO2-brine relative permeability in sandstones." Energy Procedia 63 (2014), pp. 5577-5585.

Richardson, S., B. Gao, E. Lyons, D. Magzymov, L. Poore, G. Besil, and L. Lun (2025). "Steady-state supercritical CO2 and brine relative permeability measurements at different pressure conditions." Petrophysics-The SPWLA Journal, Vol. 66, No. 01, pp. 44-53.

Sigmund, P. M. and McCaffery, F. G. (1979). "An Improved Unsteady-State Procedure for Determining the Relative-Permeability Characteristics of Heterogeneous Porous Media," Society of

Petroleum Engineers Journal, February 1979, pp. 15-28.

Wang, H., V. Alvarado, D.A. Bagdonas, J.F. McLaughlin, J.P. Kaszuba, D. Grana, E. Campbell, and K. Ng (2021). "Effect of CO2-brine-rock reactions on pore architecture and permeability in dolostone: Implications for CO2 storage and EOR." International Journal of Greenhouse Gas Control, 107: 103283.

Watson, A. T., P.C. Richmond, P.D. Kerig and T.M. Tao (1988). "A Regression-Based Method for Estimating Relative-Permeabilities from Displacement Experiments," SPE Reservoir Engineering, August, pp. 953-958.

Wyckoff, R. D. and H.G. Botset, (1936). "The Flow of Gas-Liquid Mixtures Through Unconsolidated Sands," Physics, Vol. 7, September, pp. 325-345.